A-1 time scale are

$$\Delta\nu(\mathrm{H}) = 1420.405716 \pm 0.000030,$$

$$\Delta\nu(\mathrm{D}) = 327.384347 \pm 0.000005,$$

and

$$\Delta\nu(\mathrm{T}) = 1516.701386 \pm 0.000030$$

Positronium Decay in Molecular Substances*

WERNER BRANDT
Radiation Physics Laboratory, Du Pont Experimental Station, Wilmington, Delaware

AND

S. BERKO AND W. W. WALKER
Department of Physics, University of Virginia, Charlottesville, Virginia

(Received March 16, 1960)

The overlap of the positron component of the wave function of positronium (Ps) in dense molecular substances with the lattice wave function determines the 2γ annihilation rate of positrons bound in orthopositronium via electron pickup from the lattice (τ_2 decay), and in part the 2γ angular correlation. Ps acts as a probe for the dependence of one-particle wave functions in lattices on structural lattice parameters, and of radical-molecule interactions on atomic lattice parameters. To explore the sensitivity of this probe Ps wave functions are calculated for different lattice structures in the Wigner-Seitz approximation, and the dependence of τ_2 decay on lattice parameters is derived.

This dependence was tested experimentally by τ_2 measurements on carefully characterized molecular substances in different physical states. It is confirmed that the temperature and state dependence is primarily a "free volume" effect in the sense that the overlap between the Ps and lattice wave functions decreases with increasing lattice spacing. The effects of a spherical confinement on the self-annihilation rates and stability of Ps are shown to be small for radii relevant to molecular lattices.

An anomalous behavior is found for the ice-water transition, where τ_2 increases significantly despite the contraction of water between the melting point and 4°C.

I. INTRODUCTION

ON interaction with matter, positrons annihilate with electrons into γ quanta.[1] Para decay refers to the annihilation of a positron-electron pair with antiparallel spins; ortho decay to the annihilation of a pair with parallel spins. Because of selection rules, two γ quanta are emitted in para decay and three γ quanta in ortho decay. In dense substances, positrons from a β^+ emitter are estimated to be stopped in times small compared to their lifetimes.[2] In stopping, positrons can capture an electron within a narrow range of kinetic energies (Ore gap) to form the atom (e^+e^-), positronium[3] Ps, which is unstable against annihilation. Because of the short stopping times and the narrow Ore gap, the

lifetimes of positrons bound in Ps practically coincide with the Ps lifetime with respect to annihilation.

In many molecular substances, two positron lifetimes are observed. The short mean life, τ_1, is $\sim 10^{-10}$ sec and appears to be insensitive to the lattice characteristics; in most instances, τ_1 can be attributed to the para annihilation of unbound positrons and of para Ps. The long mean life, τ_2, is $\sim 10^{-9}$ sec and can depend sensitively on temperature, physical state, molecular composition, and other parameters of the material in which the positrons annihilate; τ_2 is attributed to the fast para annihilation with lattice electrons of positrons bound in ortho Ps. This process of *electron pickup*[4] shortens drastically the long lifetime of ortho Ps of $\sim 10^{-7}$ sec against ortho annihilation. Therefore, τ_2 is a measure of the lattice-Ps interaction and its dependence on lattice properties.

Aside from lifetimes, the analysis of positron decay curves yields information also on the relative intensity of the τ_1 and τ_2 processes, I_1 and I_2, and their dependence on lattice properties. More direct evidence about the detailed annihilation process in lattices can be extracted from measurements of the angular correlation of the two γ quanta created in para annihilations.

It has been a puzzle since the discovery of the tem-

* The experimental work, performed at the University of Virginia, was partly supported by the Office of Naval Research.
[1] Reviews and extensive references are given by S. De Benedetti and H. C. Corben, *Annual Review of Nuclear Science* (Annual Reviews, Inc., Palo Alto, California, 1954), Vol. 4, p. 191; S. De Benedetti, R. E. Bell, and M. Deutsch, in *Beta- and Gamma-Ray Spectroscopy*, edited by K. Siegbahn (North Holland Publishing Company, Amsterdam, 1955), pp. 672, 680, and 689; S. Berko and F. L. Hereford, Revs. Modern Phys. **28**, 299 (1956); R. A. Ferrell, Revs. Modern Phys. **28**, 308 (1956); L. Simons, *Handbuch der Physik*, edited by S. Flügge (Springer-Verlag, Berlin, 1956), Vol. 34, p. 139.
[2] R. L. Garwin, Phys. Rev. **91**, 1571 (1953); G. E. Lee-Whiting, Phys. Rev. **97**, 1557 (1955); W. Brandt, Atomic Energy Commission Nuclear Data Tab. Suppl., 1959.
[3] A. E. Ruark, Phys. Rev. **68**, 278 (1945).

[4] R. L. Garwin, Phys. Rev. **91**, 1271 (1953); M. Dresden, Phys. Rev. **93**, 1413 (1954).

perature dependence of the τ_2 decay[5] that the pickup annihilation rate decreases with increasing temperature. It is the purpose of this paper to show that this departure from the commonly encountered increase of reaction rates with temperature is a quantum mechanical effect. The de Broglie wave length of thermalized Ps atoms is 2–3 orders of magnitude larger than the dimensions of the "free volume" per molecule accessible to Ps in a typical molecular lattice. Ps in such lattices behaves much like an "injected" exciton of high mobility, with a radius comparable to intermolecular spacings. From the point of reaction kinetics, Ps may be viewed as the elementary free radical, which by its decay characteristics signifies primary radical-molecule interactions, unobstructed by extraneous chemical changes. More precisely, electron pickup depends on the overlap of the positron component of the Ps wave function with the lattice wave function; the characteristics of Ps as a free radical in the conventional sense are associated with the electron component of the Ps wave function. However, both are uniquely interrelated by normalization conditions.

Any satisfactory theory of Ps formation and decay in molecular substances must account at least for three main observations: (1) the temperature dependence of τ_2; (2) the changes of I_2/I_1, in order-disorder phase transitions; and (3) the dependence of angular correlation on temperature and phase changes. The present paper gives an ultrasimplified theory of (1) and reports experimental data designed to test this theory as far as it goes. The results show that more detailed theoretical work is warranted, which we plan to report in subsequent papers. Also, this work has shown the need and indicates areas for more experiments of high accuracy under stringent conditions of sample preparation and characterization.

II. THEORETICAL

In the nonrelativistic approximation, the spin averaged 2γ and 3γ annihilation rates, γ_2 and γ_3, of a positron and an electron in para or ortho spin orientation, re-

spectively, are given by [1,6]

$$\gamma_2 = \pi r_0^2 c |\Psi_-(\mathbf{r}_+)|^2, \qquad (1)$$

$$\gamma_3 = \gamma_2/372, \qquad (2)$$

where $r_0 = 2.8 \times 10^{-13}$ cm and c the velocity of light. The squared term stands for the density of the electron at the position of the positron. In a lattice L of electron density distribution $|\Psi_L(\mathbf{r})|^2$ composed of neutral atoms or molecules with closed shells, i.e., in the absence of paramagnetic impurities, the electron pickup rate, γ_p, of ortho Ps in L becomes

$$\gamma_p = \pi r_0^2 c \int_L \Psi_L^*(\mathbf{r}) \Psi_{+b}^*(\mathbf{r}) \Psi_{+b}(\mathbf{r}) \Psi_L(\mathbf{r}) d\mathbf{r}^3, \qquad (3)$$

where Ψ_{+b} is the wave function of the positron in the field of the electron to which it is bound as ortho Ps and the field of the lattice. The theoretical problem is to evaluate (3) as a function of the properties of L.

The density distribution of Ps in a lattice in the lowest diffusion band is indicated schematically in Fig. 1. To explore the sensitivity of γ_p to changes in the lattice parameters, we solve Eq. (3) for the following ultrasimplified model. (1) The mutual Ps and lattice polarization is neglected; (2) the lattice constituents are approximated by square potentials of height U_0, electron density ρ_0, and radius r_0 or, correspondingly, "excluded volume" v_0, each centered in a cell volume v_1 of radius r_1. For $r_0 \le r \le r_1$, $U_1 = 0$ and $\rho_1 = 0$; $v_1 - v_0$ is the "free volume" of the cell, and $v^* = v_1/v_0$ the reduced cell volume; (3) the Ps atoms are thermalized and can be treated in the zero-velocity ($\mathbf{k}_{Ps} \simeq 0$) approximation. Setting

$$\Psi_{+b}(\mathbf{r}_+) = \alpha(\mathbf{r}_{+0}) \Psi_{Ps}(\mathbf{r}_0), \qquad (4)$$

where α is a polarization function and the subscript 0 refers to the Ps center of mass, our model assumes $\alpha = 1$. Eq. (3) becomes

$$\gamma_p = \pi r_0^2 c \rho_0 \int_{v_0} \Psi_{Ps}^* \Psi_{Ps} d\mathbf{r}^3. \qquad (5)$$

We evaluate Eq. (5) in the Wigner-Seitz approximation. With the notation

$$\Psi_{Ps} = \Phi_\mu, \quad \begin{cases} \mu = 0 & \text{for } r \le r_0, \\ \mu = 1 & \text{for } r_0 < r \le r_1, \end{cases} \qquad (6)$$

the Schrödinger equations for the excluded and the free volumes expressed in terms of an appropriate geometry are

$$[\nabla^2 - (4m/\hbar^2)(U_\mu - E)]\Phi_\mu = 0, \quad \mu = 0, 1, \qquad (7)$$

subject to the boundary conditions

$$\Phi_0(r_0) = \Phi_1(r_0),$$

$$\Phi_0'(r_0) = \Phi_1'(r_0), \qquad (8)$$
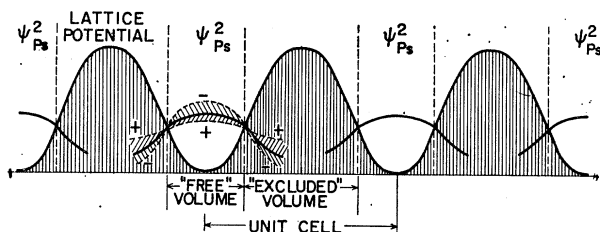
$$\Phi_1'(r_1) = 0.$$

Fig. 1. Ps density distribution (solid line) and the distributions of the positron (+) and electron (−) densities (dashed curves) in Ps polarized by the lattice (schematic).

[5] R. E. Bell and R. L. Graham, Phys. Rev. 90, 644 (1953).

[6] F. A. M. Dirac, Proc. Cambridge Phil. Soc. 26, 361 (1930).

We set

$$\Phi_\mu = \sum_{\nu=0}^{1} a_{\mu\nu} Z_{\mu\nu}, \qquad (9)$$

where the $a_{\mu\nu}$ are constants; $\nu = 0$ denotes the even and $\nu = 1$ the odd solution of Eq. (7) with regard to $r = 0$. Because of symmetry, $a_{01} = 0$. Introducing

$$C(x,y) = Z_{0c}'(x)Z_{01}(y) - Z_{00}(y)Z_{01}'(x),$$
$$C'(x,y) = Z_{00}'(x)Z_{01}'(y) - Z_{00}'(y)Z_{01}'(x), \qquad (10)$$

we have by Eq. (8)

$$\Phi_0 = a_{00}Z_{00}(r), \qquad (11)$$
$$\Phi_1 = a_{00}Z_{00}(r_0)C(r_1,r)/C(r_1,r_0),$$

subject to the compatibility condition

$$Z_{00}'(r_0)/Z_{00}(r_0) = C'(r_1,r_0)/C(r_1,r_0), \qquad (12)$$

under which we evaluate the function

$$F(U_0,r_0,r_1) =$$

$$\frac{Z_{00}{}^*(r_0)Z_{00}(r_0) \quad \displaystyle\int_{v_1} C^*(r_1,r)C(r_1,r)dr^3}{\displaystyle\int_{v_0} Z_{00}{}^*(r)Z_{00}(r)dr^3 \quad C^*(r_1,r_0)C(r_1,r_0)}. \qquad (13)$$

Introducing F in Eq. (5), γ_p becomes

$$\gamma_p = \frac{\pi r_0^2 c \rho_0}{1 + F(U_0,r_0,r_1)}. \qquad (14)$$

It should be noted that temperature does not appear explicitly in Eq. (14), because F is calculated in the $k_{Ps} = 0$ approximation and the lattice is assumed to be adiabatically rigid.

F was evaluated for the planar geometry of layer lattices, the special geometry of hard-sphere lattices, and the cylindrical geometry of chain lattices, as listed in Table I. Figures 2–4 show the dependence of F on v^* as a function of the scattering parameter
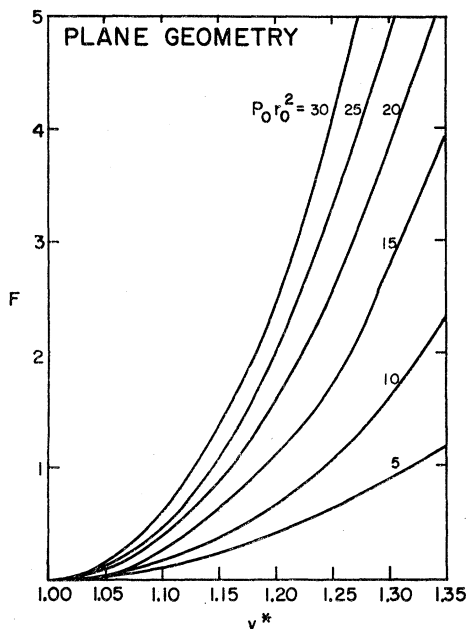
$$P_0 r_0^2 = (4m/\hbar^2)U_0 r_0^2. \qquad (15)$$

III. EXPERIMENTAL

The apparatus for positron lifetime determinations was similar to that described by Bell and Graham.[5] It consisted of a Na[22] positron source surrounded by the sample kept in a temperature bath, and a coincidence circuit. The latter records the counting rate as a function of the time-delay between the 1.28-Mev γ quantum associated with the positron emission, and one of the 0.5-Mev annihilation quanta.

The Na[22] source was deposited between films of "Mylar" polyester film. It was estimated that less than 5% of the positrons annihilated in the "Mylar" films. This sandwich was surrounded by the samples to

TABLE I. Compatibility relation, Eq. (12), and the pickup function $F(P_0r_0^2, v^*)$, Eq. (13), for different lattice geometries.

| Geometry	Plane	Sphere	Cylinder
Compatibility Eq. (12)	$(v^*-1)\eta \tanh\eta - \xi \tan\xi = 0,$	$\xi_0 \coth\xi_0 - 1 + \dfrac{(\eta_1\eta_0+1)\sin(\eta_0-\eta_1)-(\eta_0-\eta_1)\cos(\eta_0-\eta_1)}{\eta_1\cos(\eta_0-\eta_1)+\sin(\eta_0-\eta_1)} = 0,$	$\dfrac{I_1(\xi_0)}{\xi_0 I_0(\xi_0)} + \eta_0 \dfrac{G_1(\eta_0)}{G_0(\eta_0)} = 0,$
	where $\eta = \left[P_0r_0^2 - \dfrac{\xi_0^2}{(v^*-1)^2}\right]^{\frac12}$	where $\eta_0 = (P_0r_0^2 - \xi_0^2)^{\frac12},$ $\eta_1 = \eta_0 v^{*\frac13}$	where $G_0(\eta) = Y_1(\eta_1)J_0(\eta) - J_1(\eta_1)Y_0(\eta),$ $G_1(\eta) = Y_1(\eta_1)J_1(\eta) - J_1(\eta_1)Y_1(\eta),$ $I_0, I_1 = $ modified Bessel functions, $J_0, J_1 = $ Bessel functions of first kind, $Y_0, Y_1 = $ Bessel functions of second kind, $\eta_0 = (P_0r_0^2 - \xi_0^2)^{\frac12},$ $\eta_1 = \eta_0 v^{*\frac13}$
$F(P_0r_0^2, v^*)$ Eq. (13)	$\dfrac{\tan^2\xi}{\tanh^2\eta} \dfrac{1+(2\xi/\sin 2\xi)}{1+(2\eta/\sinh 2\eta)}$	$\dfrac{1}{2} \dfrac{\xi_0 \cosh(2\xi_0)-1}{\eta_0 \sinh(2\xi_0)-2\xi_0} \times$ $\dfrac{(1-\eta_1^2)\sin 2(\eta_0-\eta_1)+2\eta_1\cos 2(\eta_0-\eta_1)-\eta_0(1+\eta_1^2)-\eta_1(1-\eta_1^2)}{\eta_1\sin 2(\eta_0-\eta_1)+1-(1-\eta_1^2)\cos^2(\eta_0-\eta_1)}$	$\dfrac{\xi_0^2}{\eta_0^3} \dfrac{I_0^2(\xi_0)}{I_0^2(\xi_0)-I_1^2(\xi_0)} \times$ $\dfrac{\eta_1^2[G_0^2(\eta_1)+G_1^2(\eta_0)]-\eta_0^2 G_0^2(\eta_0)}{G_0^2(\eta_0)}$

FIG. 2. $F-v^*$ dependence in layer lattice.

be studied. For interpretation of the delay curves, the prompt resolution curve of the coincidence circuit is needed. This was obtained by measuring the annihilation rate in Al and then correcting for the positron mean life in Al, as measured by Bell and Graham ($\sim 1.5 \times 10^{-10}$ sec).

The long mean life τ_2 is obtained from the counting-rate vs delay-cable curve by standard methods. The slope of a straight line was fitted to the straight right-
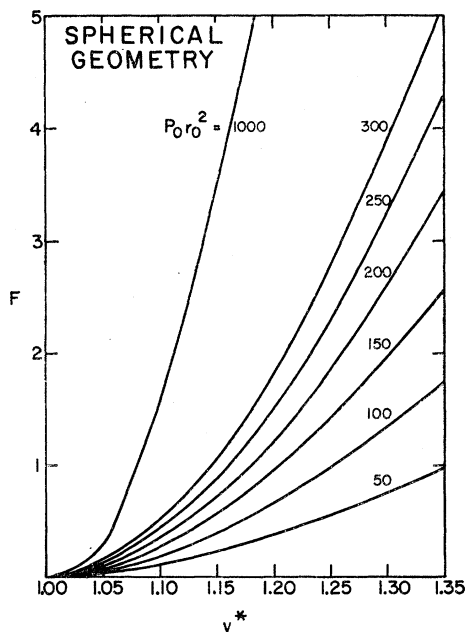
FIG. 3. $F-v^*$ dependence in hard-sphere lattice.

hand portion of the log counting-rate curve. The resolution curve was then folded into the exponential of τ_2 and the resulting curve fitted at the tail to the experimental curve. Subtraction of this folded exponential form from the experimental curve yielded the decay curve for the component annihilating with the short mean life τ_1. The ratios of the areas under these two curves gives the ratio I_1/I_2 of the τ_1 and τ_2 components.

The low-temperature measurements were performed by lowering the samples into a thin-walled Dewar vessel designed so as to allow the phototube to be positioned close to the samples. Temperatures could be held constant to less than $0.1°$ over a temperature range from $4°K$ to $400°K$.
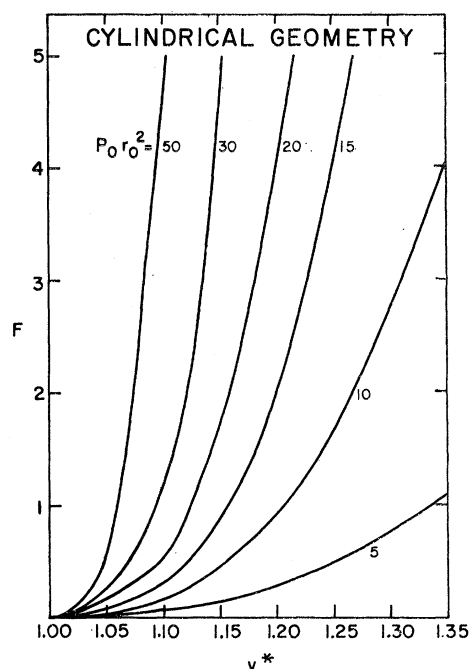
FIG. 4. $F-v^*$ dependence in chain lattice.

Each sample was measured repeatedly, and the results averaged. The errors indicated in the figures below for the τ_2 lifetimes are larger than expected from counting statistics alone. They include conservative estimates of fluctuations due to other causes. The Al curve was checked repeatedly during the measurements to insure the stability of the coincidence circuit.

In view of the theoretical results presented in Sec. II, the sample selection and preparation was made such as to vary, as independently as possible, the free volume, the temperature, and the molecular potential.

Polytetrafluoroethylene, $(-CF_2-)_n$, is known to show large variations of τ_2 with temperature. The electronic levels of paraffinic molecules are affected very little by condensation from the gas phase and by density changes in condensed phases. Therefore, polytetrafluoroethylene is a substance well suited for

studying free volume vs temperature effects, at constant molecular potential. Samples were prepared from experimental polytetrafluoroethylene resins of low and high degree of polymerization. The low-molecular-weight material can be made to crystallize to a higher degree than the high-molecular-weight material. The samples were subjected to different heat treatments to produce variations of crystallinity in the polymer lattice. Crystallinities ranging from 50 to 80% by volume were obtained, as determined by x-ray diffraction.

The Ps lifetimes in polytetrafluoroethylene are shown in Fig. 5, supplemented with data by Bell and Graham,[5] and Berko and Landes[7] assuming the polymer densities of the samples measured by the former authors to be those of commercially available polytetrafluoroethylenes.
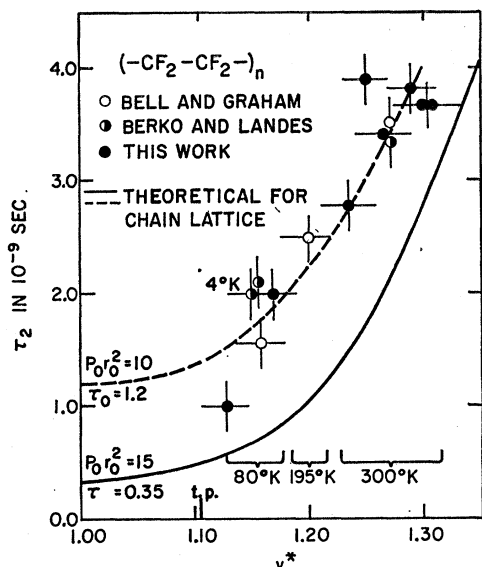
FIG. 5. τ_2 dependence on v^* in polytetrafluoroethylene.

A careful search for changes in τ_2 decay in the lattice transitions of polytetrafluoroethylene near room temperature[8] was negative.

For possible changes in the molecular potential induced by free volume changes or phase transitions, glycerol and water as substances with substantial hydrogen bonding were measured. The electronic charge distribution of atomic groups interlinked by hydrogen bonds is well known to depend on the spacing between the hydrogen-bonded groups.[9] The data are shown in Figs. 6 and 7.[10]

[7] H. S. Landes, thesis, University of Virginia, 1957 (unpublished).

[8] G. P. Furukawa, R. E. McCoskey, and G. J. King, J. Research Natl. Bur. Standards 49, 273 (1952).

[9] R. C. Lord and R. E. Merrifield, J. Chem. Phys. 21, 166 (1953).

[10] The authors would like to thank Dr. G. J. Sloan for the preparation of the crystalline glycerol, and Mr. W. S. Walker for an independent set of τ_2 data on ice-water.
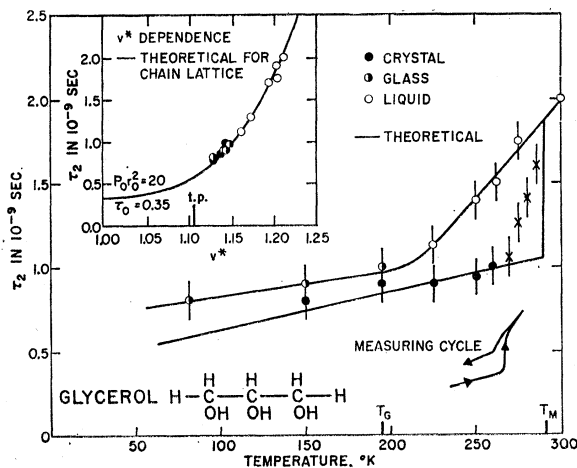
FIG. 6. τ_2 dependence on v^* and T in glycerol.

IV. DISCUSSION

The Ps mean life τ_2 is related to γ_p by

$$\tau_2^{-1} = \gamma_p + \gamma_3. \qquad (16)$$

As shown in the Appendix, the confinement of ortho Ps in a lattice will not change γ_3 significantly relative to its value for free ortho Ps, so that in the cases of interest here, $\gamma_3 \ll \gamma_p$. To this approximation and with the abbreviation $\tau_1 = (\pi r_0^2 c \rho_0)^{-1}$, Eq. (16) with Eq. (14) becomes

$$\tau_2 = \tau_0 [1 + F(P_0 r_0^2, v^*)]. \qquad (17)$$

We note that in the geometries considered for given $P_0 r_0^2$ the increase of F, and hence τ_2, with v^* is the largest in the cylindrical geometry. If r_0 is expressed in angstroms, $U_0(\text{ev}) = 1.91 (P_0 r_0^2)/r_0^2$. For discussing the experimental results in terms of Eq. (17), assumptions have to be made about τ_0 and v_0. For definiteness, we have chosen $\tau_0 = 0.35 \times 10^{-9}$ sec, the mean life of Ps$^-$, and, for calculating v^* from the equation of state
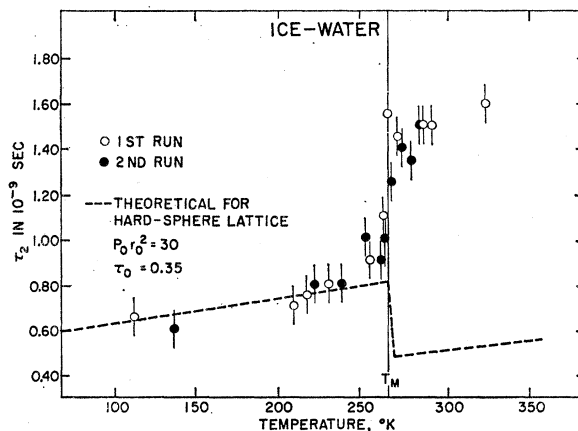
FIG. 7. τ_2 dependence on T in water.

of a substance, the relations

$$v^*(T=0)=v_1(T=0)/v_0$$

$$=\begin{cases} 3\sqrt{2}/\pi \text{ for spherical geometry} \\ 2\sqrt{3}/\pi \text{ for cylindrical geometry} \end{cases} \quad (18)$$

as the conditions for tightest packing (t.p.); $v_1(T=0)$ is the specific volume at $T=0°K$.

Figure 5 shows the volume dependence of τ_2 for polytetrafluoroethylene calculated for the cylindrical geometry of polymer lattices.[11] The experimental data comprise density variations by temperature as well as by different degrees of crystallinity. The rise of τ_2 with increasing v^* agrees satisfactorily with the theoretical curves. The uncertainty of the data exceeds whatever thermal effects one estimates to occur above and beyond the free volume changes. The fraction of annihilations in τ_2 decay, I_2, was nearly constant at $(30\pm5)\%$.

The analogous plot for glycerol is inserted in Fig. 6.[12] I_2 was $\sim(35\pm5)\%$ and temperature independent within these limits. It shows that within the accuracy of the present data, the τ_2 variations are independent of the physical state of the sample. They depend only on v^*, and parametrically on a constant $P_0 r_0^2$. The main diagram in Fig. 6 displays the theoretical curve and the experimental data as a function of temperature. The glass temperature T_G is marked by a pronounced change in slope in the glass transformation region. We attribute the sluggish rise of the τ_2 values in the melting region of glycerol (indicated by ✗) to a melting point depression by water absorption from the surrounding atmosphere in a surface layer of our crystalline samples, comparable in thickness to the range of positrons. It would be desirable to remeasure this transition under the complete exclusion of water to confirm the predicted sharp rise at the melting point.

The large and sharp rise of τ_2 at the melting point of naphthalene[13] can be accounted for completely by Eq. (17), in terms of the density change of naphthalene on melting.

By our analysis the ice-water transition shows a remarkable anomaly. As shown in Fig. 7, τ_2 in ice increases with temperature as expected. But rather than falling to minimum near 4°C on melting, τ_2 rises sharply. Concurrently, I_2 drops from $(45\pm5)\%$ in ice to $(25\pm5)\%$ in water. The possibility of this behavior was pointed out by de Zafra and Joyner[14] on the basis of Bell and Graham's first observation of this τ_2 rise on melting.[5] The τ_2-T curve begins to level off near 10°C, and approaches a temperature coefficient in agreement with the thermal expansion of water near 70°C. By contrast, the 2γ angular correlation shows a "normal" density dependence.[14] We have no satis-

factory explanation for the sudden rise of τ_2 on melting. In the framework of the present model, it could be accommodated only by a significant change in $P_0 r_0^2$ or ρ_0 on melting. It can be accounted for also by the Eucken model of a two-component water system,[15,16] in which a dynamic equilibrium exists between liquid water and crystalline water, which shifts toward the former as the temperature approaches the boiling point. Using Eucken's thermal equilibrium coefficients and the equilibrium constants given by Smith and Lawson,[17] one can reproduce the experimental rise of τ_2 on melting by assuming that the Ps wave function distributes itself between the two water components, and that the effective ρ_0 in the overlap of the Ps and H_2O wave functions in liquid water is lower than in crystalline water. Although this result appears reasonable, too little is known as yet about the changes in the H_2O wave function on melting and the dynamic molecular properties of liquid water,[18] to support such explanation by independent data. It would be desirable to measure the τ_2 vs T curve of water as a function of pressure, to separate the dynamic effects from the free volume effects.

V. SUMMARY

The temperature and phase dependence of τ_2 in molecular substances is primarily a "free volume" effect, in that the overlap between the Ps and lattice wave functions decreases with increasing lattice spacing. This predicts a concurrent narrowing of the wide component of the 2γ angular correlation, because electron pickup occurs more from the (outer) low-momentum regions of the atomic wave functions as the free volume increases.

An anomalous behavior is found for the ice-water transition, where τ_2 increases and I_2 decreases significantly despite the contraction of water on melting.

APPENDIX

The electron pickup mechanism is based essentially on the assumption that the Ps wave function in a lattice is not deformed to such an extent that Ps becomes pressure self-quenched or unstable. The effect of a confinement on the Ps ground state and hence on its self-annihilation rate can be estimated by calculating the Ps wave function in an impenetrable sphere of radius R. The effects of such confinement on the energy levels of hydrogen have been studied by several authors.[19]

[11] W. Brandt, J. Chem. Phys. 26, 262 (1957).

[12] The v^* conversion is based on the density-temperature diagram by A. K. Schulz, J. chim. phys. 51, 530 (1954).

[13] H. S. Landes, S. Berko, and A. J. Zuchelli, Phys. Rev. 103, 828 (1956).

[14] R. L. de Zafra and W. T. Joyner, Phys. Rev. 112, 19 (1958).

[15] A. Eucken, Nachr. Ges. Wiss. Göttingen 1, 38 (1946); Z. Elektrochem. 52, 255 (1948); 53, 102 (1949).

[16] L. Hall, Phys. Rev. 73, 775 (1948).

[17] A. H. Smith and A. W. Lawson, J. Chem. Phys. 22, 351 (1954).

[18] See, e.g., R. N. Brockhouse, Phys. Rev. Letters 2, 287 (1959); D. J. Hughes, H. Palevsky, W. Kley, and E. Turkelo, Phys. Rev. Letters 3, 91 (1959).

[19] A. Michels, J. de Boer, and A. Bijl, Physica 4, 981 (1937); A. Sommerfeld and H. Welker, Ann. Physik 32, 56 (1938); S. R. de Groot and C. A. Ten Seldam, Physica 12, 669 (1946); A. C. Ten Seldam, thesis, University of Utrecht, 1953 (unpublished).

We separate the Ps wave function Ψ_{+-} in center-of-mass coordinates $\mathbf{r}_0$ and relative coordinates $\mathbf{r}$:

$$\Psi_{+-}(\mathbf{r}_+,\mathbf{r}_-) = \Psi_{Ps}(\mathbf{r}_0)\,\varphi_{+-}(\mathbf{r}). \qquad (19)$$

The Ps atom is placed in the sphere such that the ground-state solution of the radial Schrödinger equation in relative coordinates complies with the boundary conditions $\varphi_{+-}(0) = $ finite and $\varphi_{+-}(R) = 0$. The solution can be written in the form

$$\varphi_{+-}(R,r) = N(R)f(R,r)\,\exp\{-r/[1+\beta(R)]\}, \qquad (20)$$

where $N(R)$ is the normalization constant. The radii R, r are given in units of $a_\mu = \hbar^2/\mu e^2$, with $\mu = m_+ m_-/(m_+ + m_-)$; for Ps, $\mu = m_e/2$. As long as $\beta \ll 1$, the functions $f(R,r)$ and $\beta(R)$ are given by

$$f(R,r) = 1 - \beta(R) \sum_{m=2}^{\infty} \frac{2^{m-1}r^{m-1}}{(m-1)m!}, \qquad (21)$$

$$\beta^{-1}(R) = \sum_{n=2}^{\infty} \frac{2^{n-1}R^{n-1}}{(n-1)n!}. \qquad (22)$$

According to Eq. (3), the self-annihilation rate of Ps is proportional to

$$\varphi_{+-}^2(R,0) = \left\{ 4\pi \int_0^R f^2(R,r) \right.$$
$$\left. \times \exp[-2r/1+\beta(R)]r^2 dr \right\}^{-1}. \qquad (23)$$

For $R \to \infty$, $\beta \to 0$ and $f(R,r) \to 1$, and Eq. (23) reduces to

$$\varphi_{+-}^2(\infty,0) = \pi^{-1}(\text{units } a_\mu^{-3}), \qquad (24)$$

which is equal to the expression $|\Psi_-(\mathbf{r}_+)|^2$, Eq. (1), for the ground state of free Ps. Consequently, the lifetime of Ps in an impenetrable sphere of radius R, τ_R, relative to that of free Ps, τ_∞, is given by

$$\frac{\tau_R}{\tau_\infty} = 4 \int_0^R f^2(R,r)\,\exp[-2r/1+\beta(R)]r^2 dr. \qquad (25)$$

The ground-state energy, E_R, relative to the ionization energy of free Ps, $E_\infty = -e^2/2a_\mu$, for $\beta \ll 1$ is given by

$$E_R/E_\infty \simeq 1 - 2\beta(R). \qquad (26)$$

TABLE II. Properties of Ps confined in impenetrable sphere.

R (unit a_μ)[a]	$\beta \times 10^3$	$(\tau_R/\tau_\infty)_{2,3\gamma}$	E_R/E_∞[a]	$p \times 10^{-3}$ (atm)	E_0(ev)
3	52.5	0.748	0.895	10.966	0.465
4	14.8	0.900	0.970	1.843	0.262
5	3.45	0.969	0.993	0.304	0.168
6	0.73	0.992	0.999	0.044	0.117
7	0.138	0.998	1.000	0.007	0.086
8	0.026	0.999	1.000	0.001	0.066
∞	0.000	1.000	1.000	0.000	0.000

[a] For Ps, $a_\mu = 1.058$ A and $E_\infty = (1/2)$ry.

The pressure, p, exerted by the Ps atom on the confining sphere becomes

$$p = -(4\pi a_\mu^3 R^2)^{-1}\left(\frac{dE}{dR}\right) \sim \frac{e^2}{8\pi a_\mu^4}\frac{\beta^2}{1+\beta}\frac{e^{2R}}{R^4}. \qquad (27)$$

The zero-point energy of the Ps in the spherical confinement is $(M = m_+ + m_-)$

$$E_0(R) = \pi^2\hbar^2/8Ma_\mu^2 R^2. \qquad (28)$$

The properties of Ps in a sphere as given by Eqs. (25)–(28) were calculated as a function of R (unit a_μ) with the corresponding β values given in reference 19, as listed in Table II. The lifetimes of ortho and para Ps are not reduced by more than 30% in confinements of dimensions comparable to intermolecular distances. This constitutes an upper limit, however, because in small confinements the pressure exerted by the Ps on the lattice would exceed the internal lattice pressure which ranges from $(2\text{–}8) \times 10^3$ atm; i.e., the confining molecules would yield before they could retain Ps in such small volumes. Neglecting polarization effects, which will be large only in strongly polar lattices, the ground-state energy is decreased by just a few percent, so that the Ps stability is not changed significantly. The last column of Table II indicates, in view of what has just been said, that the confinement in a lattice *per se* cannot be invoked for explaining the width of the 2γ angular correlation, θ, which normally corresponds to an energy $E = mc^2\theta^2/4 \simeq 0.25$ ev.[14]

Specifically, however, Table II substantiates the assumption underlying the pickup mechanism that the 3γ self-annihilation rate and the stability of ortho Ps in a molecular lattice are not altered significantly relative to ortho Ps in vacuo.